Published online 17 December 2010 *Nucleic Acids Research, 2011, Vol. 39, No. 8* ***3373–3387***
doi:10.1093/nar/gkq1247

Folding of the lysine riboswitch: importance of peripheral elements for transcriptional regulation

Simon Blouin, Raja Chinnappan and Daniel A. Lafontaine*

Groupe ARN/RNA Group, Département de biologie, Faculté des sciences, Université de Sherbrooke, Sherbrooke, Québec, Canada, J1K 2R1

Received July 23, 2010; Revised October 21, 2010; Accepted November 17, 2010

ABSTRACT

The *Bacillus subtilis lysC* lysine riboswitch modulates its own gene expression upon lysine binding through a transcription attenuation mechanism. The riboswitch aptamer is organized around a single five-way junction that provides the scaffold for two long-range tertiary interactions (loop L2–loop L3 and helix P2–loop L4)—all of this for the creation of a specific lysine binding site. We have determined that the interaction P2–L4 is particularly important for the organization of the ligand-binding site and for the riboswitch transcription attenuation control. Moreover, we have observed that a folding synergy between L2–L3 and P2–L4 allows both interactions to fold at lower magnesium ion concentrations. The P2–L4 interaction is also critical for the close juxtaposition involving stems P1 and P5. This is facilitated by the presence of lysine, suggesting an active role of the ligand in the folding transition. We also show that a previously uncharacterized stem–loop located in the expression platform is highly important for the riboswitch activity. Thus, folding elements located in the aptamer and the expression platform both influence the lysine riboswitch gene regulation.

INTRODUCTION

Riboswitches are genetic control elements located in untranslated regions of mRNA that positively or negatively modulate messenger RNA (mRNA) cellular levels, mostly through conformational changes. Riboswitches have been found in all kingdoms of life and shown to regulate gene expression by transcription attenuation, translation initiation, ribozyme-mediated mRNA processing and mRNA splicing (1). These RNA regulatory elements directly bind cellular metabolites and alter the expression of downstream genes that are usually associated with the biosynthesis or transport of target metabolites (2–4). The riboswitch-driven genetic control can also be initiated through a number of cellular factors, such as magnesium ions (5), temperature (6) and uncharged tRNA (7).

Riboswitches are composed of two modular domains: an aptamer and an expression platform. The most conserved region of riboswitches is the aptamer, which is a receptor that specifically binds a target metabolite. However, the expression platform varies widely in sequence and structure and typically affects gene expression through secondary structure reorganization. Switching between gene activation and repression is accomplished by the ligand-induced riboswitch reorganization, which adopts mutually exclusive secondary structures (8,9). Recently, several bioinformatic studies have provided strong support for putative additional RNA regulatory elements that still await characterization (10–15).

In the bacterium *Bacillus subtilis*, two riboswitches are involved in the regulation of the lysine cellular level by controlling the expression of an aspartokinase II (*lysC*) and a lysine transporter (*yvsH*) (16–18). Lysine binding to the *lysC* riboswitch was shown to cause structural changes in the aptamer domain and to downregulate gene expression by transcription attenuation (16,17). The lysine riboswitch secondary structure is based on conserved elements previously shown to be reorganized upon lysine binding (Figure 1A)—leading to the anti-antiterminator (P1) stem stabilization and transcription attenuation (16,17,19,20). Recently, lysine riboswitch crystal structures have shown that the riboswitch aptamer is organized around a five-way junction (19,20) with helical stacking occurring between stems P1 and P2 and between stems P4 and P5 (Figure 1A). Both stacks are arranged in an X conformation commonly observed for RNA four-way junctions, where a close juxtaposition is observed between P1 and P5 for the lysine aptamer. The global fold of the riboswitch is defined by the presence of long-range tertiary interactions occurring between loops L2–L3 (L2–L3) and helix P2–loop L4 (P2–L4). The L2–L3 loop–loop interaction was previously shown to be

*To whom correspondence should be addressed. Tel: +819 821 8000; Fax: +819 821 8049; Email: daniel.lafontaine@usherbrooke.ca

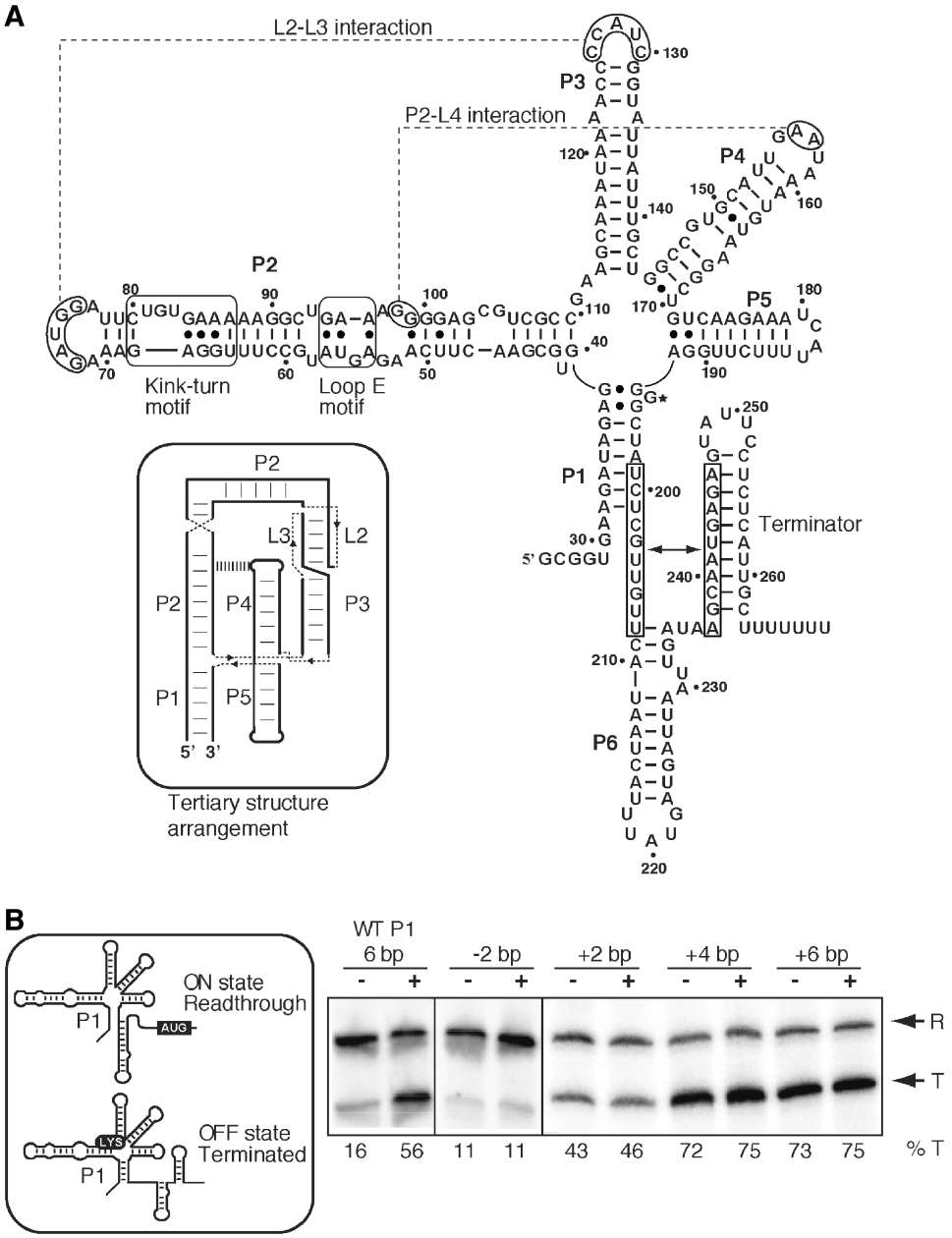

Figure 1. Secondary structure and activity of the lysine riboswitch as a function of lysine. (**A**) Secondary structure representing the lysine riboswitch. Regions involved in the formation of the kink–turn, loop E and terminator are indicated (16–21). Loop–loop L2–L3 and helix–loop P2–L4 interactions are shown by dotted lines and regions involved in the formation of the antiterminator are boxed and indicated by an arrow. Position 194 where a 2AP is introduced is shown by a star. The tertiary structure arrangement is shown in the inset, where discontinuities in the single-stranded regions are represented by dashed lines. The P2–L4 interaction is represented by vertical lines. (**B**) Single-round *in vitro* transcriptions performed as a function of P1 length in absence (–) or in presence (+) of 5 mM lysine. Variations in the total number of base pairs in P1 are indicated. Readthrough and prematurely terminated transcripts are indicated on the right and the percentage of termination is indicated below each reaction lane. Both structures representing the ON and OFF states are shown in the inset where the P1 stem is stabilized in presence of lysine.

dependent of the kink–turn motif located in the P2 stem and found to be important for the riboswitch folding and transcription regulation (21). The helix–loop interaction P2–L4 was recently established from crystallographic studies and involves invariant residues of the stem P2 and the loop L4 (Figure 1A). The resulting complex architecture of the riboswitch creates a tight binding pocket that specifically recognizes both charged ends of the bound lysine, thus ensuring high discrimination against lysine structural analogs (19,20). However, due to the presence of a small cavity in the binding site, the riboswitch can accommodate the binding of antimicrobial lysine analogs carrying modifications at position C4 such as *S*-(2-aminoethyl)-L-cysteine (AEC) and L-4-oxalysine (19). Resistance to such compounds is conferred through mutations in the lysine riboswitch aptamer that disrupt critical elements in the core or tertiary interactions (22–24).

We have previously shown that the long-range interaction L2–L3 is important for the transcription regulation of the *lysC* lysine riboswitch (21). Upon the folding of a kink–turn motif located in the P2 stem, loops L2 and L3 interact to reorganize the riboswitch core and to allow premature transcription termination. Because nucleotides located in P2 and P4 directly interact with lysine (19,20), we hypothesized that the P2–L4 interaction would be of paramount importance for the lysine riboswitch function. Thus, to understand how the lysine riboswitch makes use of peripheral elements such as L2–L3 and P2–L4, a series of biophysical and biochemical assays were performed to study the role of these elements on the riboswitch folding and transcriptional activity. Our results show that the folding of either L2–L3 or P2–L4 is optimal when both interactions are functional, as observed from the Mg^{2+} concentration required to fold the aptamer. As reported for L2–L3 (21), we also find that the presence of P2–L4 is very important for the organization of the binding site and for the riboswitch activity. The P2–L4 interaction was also determined to be crucial for a folding transition occurring between stems P1 and P5, as observed in the crystal structure. Interestingly, the P5 stem was found to functionally replace the P1 stem as the anti-antiterminator, suggesting that various peripheral elements may be used to regulate riboswitch activity. Lastly, we establish that the previously uncharacterized helix P6 found in the expression platform is very important for the adoption of the ON state, indicating that folding elements located outside the aptamer region may also have a strong influence on riboswitch activity.

MATERIALS AND METHODS

Synthesis of RNA molecules

RNA molecules were transcribed from double-stranded DNA template using T7 RNA polymerase (25). Templates for transcription were made by polymerase chain reaction (PCR) from synthetic DNA oligonucleotides (Sigma Genosys, Canada). All transcribed RNA species begin with a 5′-GCG sequence to minimize the 5′-heterogeneity of the RNA population (26). RNA molecules containing 2-aminopurine (2AP) were bought from Integrated DNA Technologies (IDT) and purified as described previously (27). The internally labeled 2AP aptamers were assembled by ligation from oligonucleotides of the following sequences (all written 5′ to 3′):

5′ transcribed strand:
GCGGUGAAGAUAGAGGUGCGAACUUCAAGAG
UAUGCCUUUGGAGAAAGAUGGAUUCUGUG
AAAAAGGCUGAAAGGGGAGCGUCGCCGAAG
CAAAUAAAACCCCAUCGGUAUUAUUUGCUG
GCCGUGCAUUGAAUAAAUGUAAGGCUGUCA
AGAAGCAUC
3′ strand:
5′-PO_4-AUUGCUUCUUGGAG(2AP)GCUAUCUUCA
CC.

Mutations in the 5′ transcribed strand were also prepared with different oligonucleotides carrying sequence changes indicated in the text. Reconstituted 2AP-containing riboswitches were prepared as previously described (21). Dual-labeled riboswitches used in fluorescence resonance energy transfer (FRET) assays were prepared by annealing a 5′ transcribed strand:

GCGGUGAAGAUAGAGGUGCGAACUUCAAGAG
UAUGCCUUUGGAGAAAGAUGGAUUCUGUG
AAAAAGGCUGAAAGGGGAGCGUCGCCGAAG
CAAAUAAAACCCCAUCGGUAUUAUUUGCUG
GCCGUGCAUUGAAUAAAUGUAAGGCUGUCA
AGAAGCAUCGG
and a 3′ synthetic strand:
5′-Cy3-CCGAUGCUUCUUGGAGGGCUAUCUU
(5-N-U)CACC

RNA were bought from IDT and purified as described previously (27). The 3′ strand was internally labelled with fluorescein (Invitrogen) at the 5′-amino-allyl uridine nucleotide, according to the manufacturer's protocol. Purified 5′ and 3′ strands were annealed by heating a mixture (molar ratio 1.1:1) to 65°C in 10 mM HEPES, pH 7.5, 50 mM NaCl, 10 mM $MgCl_2$ and slowly cooled to 30°C. The complex was purified on 8% non-denaturing acrylamide:bisacrylamide (29:1) gel, electro-eluted, precipitated in ethanol and dissolved in water.

Single-round *in vitro* transcription assays

DNA templates for single-round *in vitro* transcriptions were prepared by PCR with a combination of oligonucleotides corresponding to *B. subtilis glyQS* promoter fused to *B. subtilis* lysine riboswitch and a 95-nt sequence downstream of the expression platform (21). The promoter region ends by an adenine and is fused to the C17 position of the riboswitch sequence, allowing the transcription to be initiated by the ApC dinucleotide. In the terminated species, the RNA polymerase (RNAP) stops at position 269. The readthrough species allows the RNAP to continue 95 nt further (i.e. 49 nt after the AUG). Reactions were performed and analyzed as previously described (21). Experiments have been performed at least three times and all exhibited very similar uncertainties (<6%).

2AP fluorescence spectroscopy

Fluorescence spectroscopy was performed on a Quanta Master fluorometer. All data were collected at 10°C in 90 mM Tris-borate, pH 8.3 and 100 mM KCl and analyzed as performed previously (21). Briefly, excitation for 2AP fluorescence was done at 300 nm to obtain a good separation between the Raman peak and the 2AP fluorescence signal. The fluorescence data are fitted to a simple two-state model that assumes an all-or-none conformational transition induced by the binding of magnesium ions, with a Hill coefficient n and an apparent association constant K_A. The proportion of folded aptamer (α) is given by

$$a = K_A \bullet \left[Mg^{2+}\right]^n / \left(1 + K_A \bullet \left[Mg^{2+}\right]^n\right)$$

As the parameters K_A and n co-vary, we present the $[Mg^{2+}]_{1/2} = (1/K_A)^{1/n}$, which gives a robust estimate for

the affinity of magnesium ions (27,28). Experiments have been performed at least three times and all exhibited very similar uncertainties (<5%).

FRET analysis

Fluorescence spectroscopy was performed on a Quanta Master fluorometer and spectra were corrected for lamp fluctuations and instrument variations as described (27). Polarization artifacts were avoided by setting excitation and emission polarizers crossed at 54.75°. Values of E_{FRET} were determined using the acceptor normalization method (29,30). All data were collected at 4°C in 90 mM Tris-borate, pH 8.3 and 100 mM KCl. Fluorescein and cyanine 3 fluorophores were excited at 490 and 547 nm, respectively. Data were collected using 10 pmol of fluorescent dual-labeled riboswitch and magnesium ions were titrated over the range indicated. Experiments have been performed at least three times and all exhibited very similar uncertainties (<5%).

Native gel electrophoresis

[5′-^{32}P] labeled lysine riboswitch aptamers were incubated at 70°C for 3 min and allowed to slowly cool to room temperature to ensure homogeneous folding. Samples were then electrophoresed in 90 mM Tris-borate, pH 8.3 and 1 mM $MgCl_2$ in 8% acrylamide:bisacrylamide (29:1) gel in Tris-borate buffer containing 1 mM $MgCl_2$ at room temperature at 150 V for 18 h with the running buffer circulated during the electrophoresis. The gels were exposed to PhosphorImager screens and imaged.

SHAPE analysis

Wild-type and mutant riboswitch aptamers were prepared as previously described, with the addition of the sequence GGAGCUAAAGAGAAGCGGAAG at the 3′ end to allow binding of a complementary DNA oligonucleotide primer. Each reaction was prepared using 1 pmol of purified aptamer resuspended in 2 vol of 0.5X TE buffer, in which was added 1 vol of 3.3X folding buffer containing 333 mM K-HEPES, pH 8.0, 333 mM NaCl and the desired concentration of $MgCl_2$. Samples were heated to 65°C and allowed to slowly cool to 30°C before being pre-incubated 10 min at 37°C. *N*-methylisatoic anhydride (Invitrogen) dissolved in DMSO was then added and allowed to react for 80 min at 37°C. Modified RNA was ethanol precipitated, washed with 70% ethanol and resuspended in 0.5× TE buffer. For SHAPE analysis in the presence of ligand, L-lysine (Sigma) was added to a final concentration of 5 mM, and the final 100 mM NaCl concentration was replaced by 75 mM NaCl and 25 mM KCl. Reverse transcription reactions were performed as previously described (31) and reverse transcribed products were separated on 5% denaturing polyacrylamide gel. The gels were exposed to PhosphorImager screens and imaged. Individual band intensities in Figure 3B were integrated using SAFA (32).

RESULTS

The P1 stem stability is crucial for lysine riboswitch transcription regulation

With the exception of the glmS ribozyme (33), all reported riboswitches control gene expression by modulating the formation of a helical domain, the P1 stem, which is of central importance for the folding of the expression platform and riboswitch activity. In a biological context, the P1 stem of the lysine riboswitch is not folded in absence of lysine, which allows gene transcription to occur (ON state, Figure 1B, inset). However, upon lysine binding, the P1 stem is stabilized and premature transcription termination is favored (OFF state). Examination of crystal structures suggests that the lysine riboswitch uses complex folding elements to recognize lysine and to achieve ligand-dependent P1 stem stabilization. To investigate whether P1 stem stability is sufficient for transcription attenuation or whether lysine-induced riboswitch core reorganization is required, we varied the stability of the P1 stem of the *B. subtilis lysC* lysine riboswitch and studied its effect on premature transcription termination.

Single-round *in vitro* transcriptions were carried out using a DNA template containing the *B. subtilis glyQS* promoter upstream of the lysine riboswitch and a 95-nt sequence downstream of the terminator. When performing transcription reactions using *Escherichia coli* RNAP in absence of lysine, a low transcription termination efficiency of 16% was observed (Figure 1B). However, when 5 mM lysine was present in the transcription reaction, 56% premature termination was obtained indicating that ligand binding to the lysine riboswitch modulates transcription attenuation *in vitro*, as previously reported (16,17,21,22). To investigate the influence of the P1 stem on riboswitch activity, we increased P1 length by 2 bp and observed a disrupted riboswitch regulation, regardless of the presence of the ligand (≥43%; Figure 1B). Further elongation of the P1 stem by 4 bp and 6 bp yielded similar high termination efficiencies (≥72%), suggesting that the riboswitch is locked in the OFF state by the high stability of P1 (Figure 1B). By contrast, when 2 bp were removed from this stem (–2 bp, Figure 1B), a reduced termination efficiency of only 11% was obtained independently of lysine's presence. Together, these results suggest that the formation of the RNA–ligand complex is not required to yield premature transcription termination. Indeed, the modulation of the P1 stem stability is sufficient to lock the riboswitch either in the ON or OFF state, resulting in significant differences in basal expression levels.

The P2–L4 interaction is important for *lysC* riboswitch activity

Our laboratory has previously shown that stem–loops P2 and P3 are involved in a loop–loop interaction that is important for the riboswitch structure (21). An additional tertiary interaction involving conserved elements from P2 and L4 has recently been discovered (19,20), which is of particular interest since both P2 and P4 stem–loops

directly interact with lysine. Thus, to determine the importance of the P2–L4 interaction for riboswitch function, a series of riboswitch constructs were analyzed using single-round *in vitro* transcription.

Adenines at positions A156 and A157 in L4 are very conserved (16–18) and interact with G98 and G99 of the P2 helical domain (Figure 1A). Deletion of A156 significantly reduced premature termination in absence as well as in presence of lysine, clearly indicating that the P2–L4 interaction is important for lysine-mediated riboswitch activity (Figure 2B). Moreover, when both adenines 156 and 157 were replaced with cytosines (L4 mutant), a similar reduction in premature termination was observed (Figure 2B), consistent with the conserved nature of these nucleotides. A similar result was obtained when introducing a G98A/G99A mutation in the P2 helical domain (P2 mutant; Figure 2B).

The importance of the P2–L4 interaction was also assessed by modulating the length of the P4 stem as we anticipated that it would preclude the P2–L4 interaction to take place. As expected, the riboswitch activity was severely compromised with a complete disruption in lysine-mediated transcription termination when the P4 stem was either reduced to 4 bp or elongated to 19 bp (Figure 2A and B). Taken together, these results are consistent with the formation of the P2–L4 tertiary interaction being functionally important for the *B. subtilis lysC* lysine riboswitch.

Long-range interactions L2–L3 and P2–L4 define the global fold of the riboswitch

The tertiary structure of the lysine riboswitch comprises the long-range tertiary interactions L2–L3 and P2–L4 that are important for the transcriptional regulation (Figure 2B and ref. 21). To investigate how interactions L2–L3 and P2–L4 influence the riboswitch global structure, we employed the native gel assay, a technique that has been used to study global conformational changes in nucleic acids (27,34–38). Given that a compact structure migrates faster than an unfolded one, which is generally more extended, we speculated that aptamers correctly folded should display a faster migration rate compared to those incorrectly folded.

Clear differences in the migration pattern in a native polyacrylamide gel with 1 mM magnesium ions were detected between wild-type and several mutants,

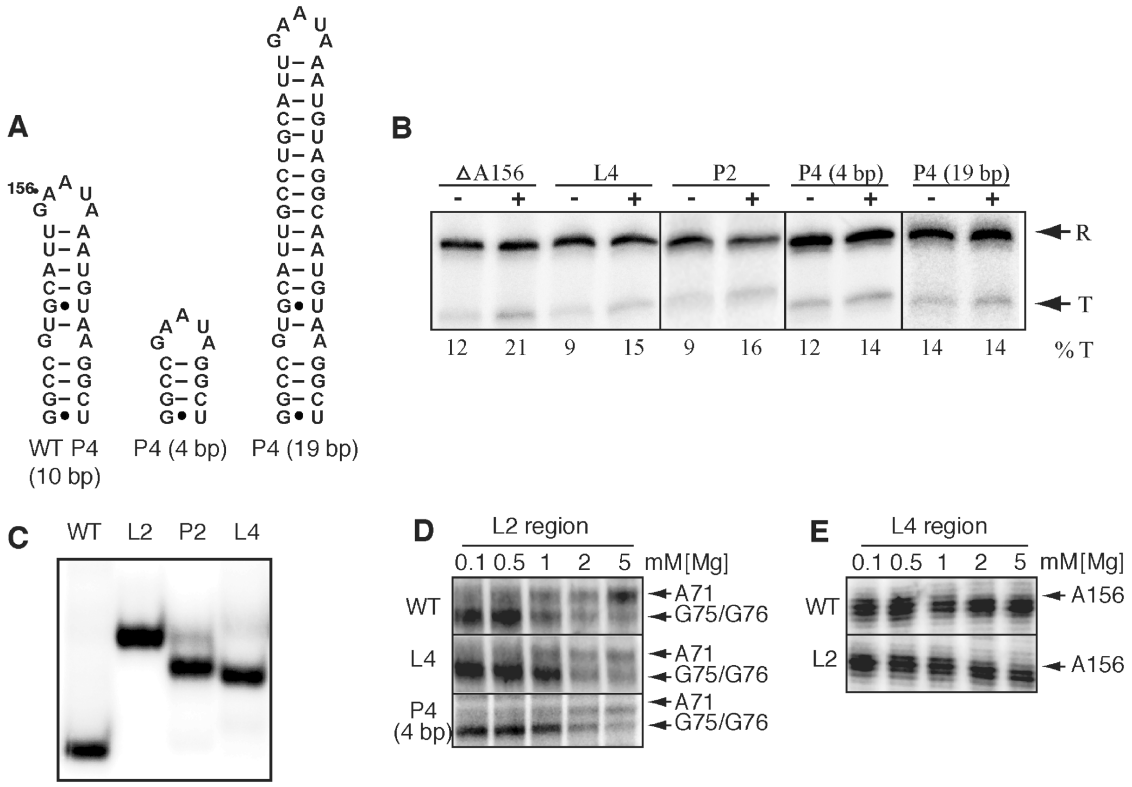

Figure 2. The P2–L4 interaction is important for the folding and activity of the riboswitch. (**A**) Secondary structure of the 4 bp and the 19 bp P4 stem mutants. (**B**) Single-round *in vitro* transcription assays made using selected P4 riboswitch mutants in absence (–) or in presence (+) of 5 mM lysine. Reactions were performed for the A156-deleted variant (ΔA156), A156C/A157C (L4), G98C/G99C (P2), P4 (4 bp) and P4 (19 bp). Readthrough (R) and prematurely terminated (T) transcripts are indicated on the right and the percentage of termination (%T) is indicated below each reaction lane. Vertical bars separate results obtained from different gels. (**C**) Non-denaturing gel electrophoresis of the wild-type (WT) and lysine aptamer mutants in the presence of 1 mM magnesium ions. The mutants L2 (G72C/A73U/U74A/G75C/G76C), P2 and L4 disrupt one of either L2–L3 or P2–L4 tertiary interactions, which results in a slower electrophoretic migration rate. (**D** and **E**) SHAPE modification of the lysine riboswitch performed at various magnesium ion concentrations. SHAPE data show that disruption of the P2–L4 interaction increases the magnesium requirement to induce the L2–L3 interaction (D) and that the disruption of the L2–L3 interaction increases the magnesium requirement to form the P2–L4 interaction (E). Arrows show SHAPE-reactive sites that are significantly modulated by magnesium ions.

suggesting a disruption in distinct tertiary structures (Figure 2C). A riboswitch aptamer having a disabled L2–L3 interaction (mutant L2) exhibited a slower migration when compared to the wild-type sequence (Figure 2C). A precedent for this migration behavior has been observed for the adenine riboswitch, where the disruption of the loop–loop interaction reduced the migration rate in native gels (27,36). Disruption of the P2–L4 interaction (P2 and L4 mutants) also reduced the aptamer migration rate, albeit not as much as the L2 mutant (Figure 2C). Thus, our results are consistent with both L2–L3 and P2–L4 tertiary interactions being important for the adoption of the global structure of the aptamer.

The L2–L3 and P2–L4 interactions are interdependently folding units

Although our native gel data suggest that both L2–L3 and P2–L4 tertiary interactions can be individually disrupted to alter the global riboswitch structure, we wanted to gain more quantitative information about the folding requirement of each interaction. We thus used selective 2′-hydroxyl acylation analyzed by primer extension (SHAPE) to obtain information about the folding of the lysine aptamer (31). This technique is particularly relevant to discriminate local nucleotide flexibility against constrained RNA regions, where 2′-hydroxyl groups in flexible regions are prone to react with electrophiles like *N*-methylisatoic anhydride (NMIA). SHAPE chemistry is therefore an excellent tool to look closely at the formation of tertiary interactions in the lysine riboswitch, as previously reported (20). When subjected to NMIA reaction as a function of Mg^{2+} concentration, the lysine riboswitch aptamer exhibited clear changes in NMIA reactivity, especially in regions involved in L2–L3 and P2–L4 long-range interactions (Supplementary Figure S1A). The relative reaction intensity was plotted as a function of Mg^{2+} to calculate the concentration required to obtain half of the change ($[Mg^{2+}]_{1/2}$; see 'Materials and Methods' section). This analysis was done for the L2, L3, P2 and L4 regions of the riboswitch that are involved in L2–L3 and P2–L4 tertiary interactions (Table 1). While L2 and L3 gave very similar results (0.82 and 0.85 mM, respectively), P2 and L4 gave slightly different $[Mg^{2+}]_{1/2}$ values (1.11 and 0.59 mM, respectively). However, partial nuclease digestion of an isolated P4 stem–loop revealed that the L4 region undergoes an independent Mg^{2+}-induced structural rearrangement, indicating that the $[Mg^{2+}]_{1/2}$ value obtained for L4 in the context of the riboswitch probably reflects multiple folding processes (Blouin,S. and Lafontaine,D.A., unpublished data). Nevertheless, SHAPE results obtained for L2, L3 and P2 regions clearly suggest that both long-range tertiary interactions fold with magnesium ions in the low mM range.

Table 1. SHAPE modification of the lysine riboswitch as a function of magnesium ions

Riboswitch region	$[Mg^{2+}]_{1/2}$ (mM)
L2[a]	0.82
P2[b]	1.11
L3[c]	0.85
L4[d]	0.59

Half of apparent concentrations for the magnesium-induced folding process ($[Mg^{2+}]_{1/2}$) were measured under standard conditions; asymptotic standard deviations on the fits indicate that errors in ($[Mg^{2+}]_{1/2}$) are generally <10% of values.
[a]Nucleotides A71, G75 and G76 were monitored.
[b]Nucleotide G98 was monitored.
[c]Nucleotide A128 was monitored.
[d]Nucleotide A156 was monitored.

We next studied the L2–L3 interaction as a function of Mg^{2+} concentration in the context of a riboswitch exhibiting a compromised P2–L4 interaction (Figure 2D). SHAPE experiments performed on both wild-type and L4 mutant molecules clearly indicated that the interaction L2–L3 required more magnesium ions to fold in absence of P2–L4. For instance, although the wild-type aptamer showed protection against NMIA reaction for positions G75/G76 in the presence of 1 mM Mg^{2+}, the L4 mutant exhibited such protection only when using 2 mM Mg^{2+} (Figure 2D). Similarly, the position A71 did not react to NMIA at 5 mM Mg^{2+} in the context of the L4 mutant, as observed for the wild-type aptamer. Very similar results were obtained when using an aptamer mutant having the P4 stem reduced to 4 bp (P4 mutant, Figure 2D).

We also analyzed the P2–L4 interaction as a function of the L2–L3 tertiary interaction (Figure 2E). Similar to our results for the L2–L3 interaction, the P2–L4 interaction also required more magnesium ions to fold when L2–L3 was disabled, as deduced from the absence of protection of A156 at 1 mM Mg^{2+}. Taken together, these results suggest that although both L2–L3 and P2–L4 interactions can fold independently of each other, they require less Mg^{2+} to form when both interactions are functional.

The G39C mutation inhibits binding without disrupting the riboswitch global folding

We and others previously characterized a riboswitch core mutation (G39C) known to cause *lysC* derepression and to severely perturb the lysine riboswitch transcriptional control *in vitro* (17,21,23,39). According to the recently crystallized riboswitch structures (19,20), G39 interacts with lysine via its 2′OH in the bound conformation. To characterize the influence of G39 on the folding of the riboswitch, we analyzed the influence of this core mutation on the lysine aptamer using native gel electrophoresis. In contrast to what we obtained when disrupting interactions L2–L3 or P2–L4, the introduction of a G39C mutation did not result in a retarded gel migration when compared to the wild-type molecule (Figure 3A), suggesting that both L2–L3 and P2–L4 interactions can form in this context.

We next studied the influence of G39C on the lysine-induced folding of the aptamer using SHAPE assays. To establish if ligand binding can assist in aptamer folding, we used a Mg^{2+} concentration of 0.5 mM that does not allow formation of interactions L2–L3 and P2–L4 (Figure 2D and E). When the wild-type molecule was subjected to NMIA reaction

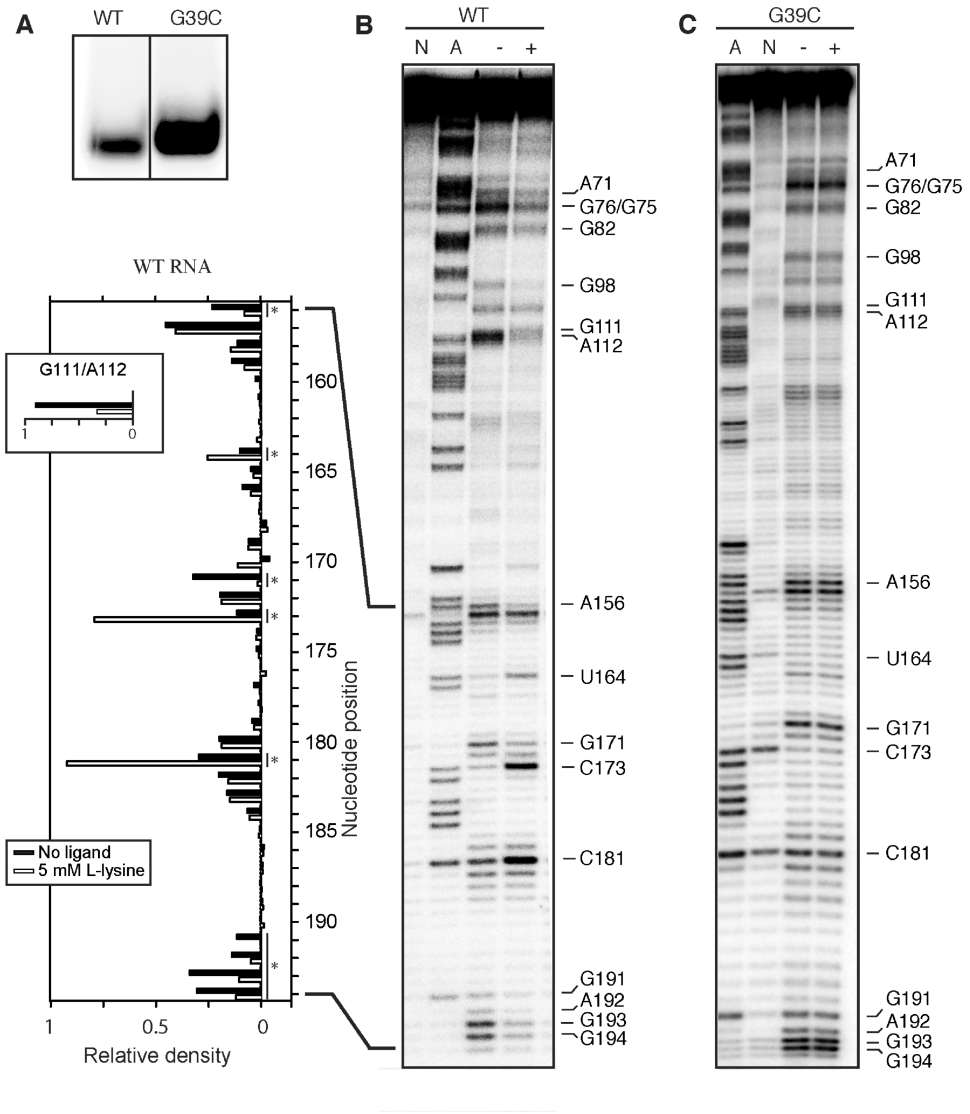

Figure 3. The G39C mutation inhibits binding without disrupting the global folding of the riboswitch. (**A**) Non-denaturing gel electrophoresis of the wild-type (WT) and G39C mutant in presence of 1 mM magnesium ions. The G39C mutant exhibits a migration similar to the wild-type, indicating that it does not perturb the global folding of the riboswitch. Note that both lanes were taken from the same gel but were manually juxtaposed to clearly indicate the co-migration of both aptamers. (**B**) SHAPE modification of the lysine riboswitch performed on the wild-type aptamer (WT). Reactions were performed at 0.5 mM $MgCl_2$, in absence (–) and in presence (+) of 5 mM L-lysine. N and A represent unreacted RNA and an adenine sequencing lane, respectively. Nucleotides of the wild-type aptamer exhibiting a lysine-induced modification are indicated on the right of the gel. The histogram on the left represents the relative density of bands corresponding to nucleotides 156–194, where filled and empty bars represent quantifications in absence and in presence of lysine, respectively. Positions showing significant difference in lysine-induced modification are marked by an asterisk. The inset represents a quantification of the reactivity of nucleotides G111 and A112. (**C**) SHAPE modification of the lysine riboswitch performed for the G39C aptamer mutant. Reactions were performed at 0.5 mM $MgCl_2$, in absence (–) and in presence (+) of 5 mM L-lysine. N and A represent unreacted RNA and an adenine sequencing lane, respectively.

using a concentration of 5 mM lysine, clear changes could be observed in regions involved in tertiary interactions L2–L3 and P2–L4 (Figure 3B). Additional reactions were observed in the aptamer core region that constitutes the lysine binding pocket, such as G111, A112 and G193 (19,20). Moreover, significant lysine-induced NMIA reactivity was obtained in the P5 stem, as previously reported (20). By contrast, the mutant G39C did not show significant changes in presence of lysine (Figure 3C), consistent with its negative effect on transcription regulation (17,21).

The P2–L4 interaction organizes the riboswitch binding pocket

We have previously employed the fluorescent local reporter 2AP to show that the formation of the L2–L3 long-range tertiary interaction is important for the lysine riboswitch core folding (21). In these studies, 2AP was introduced at the nonconserved position 194 (Figure 1A), which, according to the crystal structure of the *Thermotoga maritima* lysine riboswitch variant (19,20), is exposed to the solvent and makes stacking interaction with an extra bulged

nucleotide found in the P3 helical domain (19,20). Given that the bulged nucleotide is not present in the *B. subtilis lysC* riboswitch, it is expected that G194 does not have significant interaction with the rest of the core of the riboswitch, as suggested by its non-conserved nature.

2AP fluorescence was used to characterize the influence of the P2–L4 interaction on the folding of the riboswitch core domain. The addition of Mg^{2+} to a 2AP-labeled wild-type lysine aptamer resulted in an increase in fluorescence (Figure 4), which is consistent with position 194 being exposed to the solvent in the crystal structure (19,20). Fluorescence changes were fitted using a simple two-state transition model that allowed us to estimate values for apparent Mg^{2+}-binding parameters. With this model, an apparent affinity for magnesium ions $[Mg^{2+}]_{1/2}$ of 1.9 mM and a Hill coefficient $n = 1.6 \pm 0.1$ were obtained, suggesting that the transition exhibits a cooperative character, which is consistent with our previous findings (21). The disruption of the P2–L4 interaction (L4 mutant) severely perturbed the 2AP folding transition, as opposed to the folding of the L2–L3 interaction (Figure 2E), suggesting that the P2–L4 interaction is very important for the reorganization of the riboswitch core (Figure 4). As a comparison, we also performed the same experiment using a riboswitch having a G39C mutation that strongly inhibits riboswitch activity but that does not perturb global folding (Figure 3A). As found for the L4 mutant, almost no change in 2AP fluorescence was observed as a function of Mg^{2+}, indicating that the local folding is also strongly perturbed. Thus, together with native gel data, our 2AP fluorescence results show that formation of a P2–L4 long-range interaction is very important for riboswitch global folding and core reorganization to ensure lysine-dependent riboswitch activity (Figure 2B).

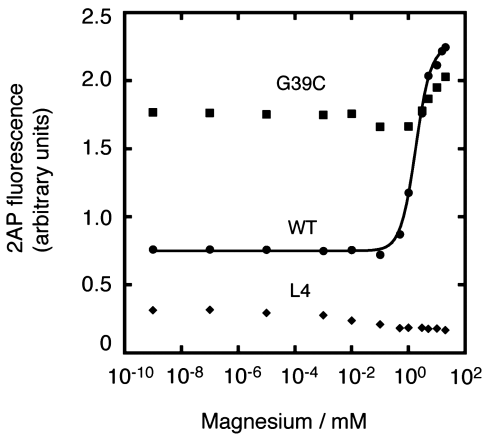

Figure 4. The formation of the P2–L4 interaction is important for riboswitch core folding. Normalized 2AP fluorescence intensity plotted as a function of magnesium ions for the WT (circles), the P2–L4-deficient L4 mutant (diamonds) and the G39C mutant (squares). The experimental data were fitted by regression to a simple two-state model where the binding of metal ions to the aptamer induces a structural change. Note that no significant change is observed when using either the L4 or G39 mutant.

The P5 stem is important for riboswitch activity

The P5 stem is the least conserved helical domain of the lysine riboswitch where only the three-first base pairs located in proximity to the junction are conserved (16–18,22). Crystal structures of the lysine riboswitch show that the P5 stem is juxtaposed to the 3′ strand of P1 (19,20). Interestingly, it has been previously reported that P5 is reactive to structural probing depending of the presence of lysine, suggesting that P5 is involved in a riboswitch structural reorganization (17,19,20). Single-round transcription assays were thus used to determine the importance of the P5 stem for the *lysC* riboswitch activity. A riboswitch construct having the P5 stem–loop reduced to 5 bp exhibited poor premature termination efficiency regardless of lysine's presence (Figure 5A and B). However, a P5 stem increased to 16 bp yielded higher premature transcription termination in absence or presence of lysine (Figure 5B). These results show that the stability of the P5 stem correlates with the riboswitch transcription termination efficiency, which is reminiscent of what we observed for the P1 stem (Figure 1B). These results suggest that P5 is important for the riboswitch regulation mechanism.

A P1–P5 folding transition is observed by FRET

Although crystal structures generate invaluable information about folded state(s) of the aptamer domain, they do not provide details regarding the structural sampling that riboswitches may experience for efficient ligand binding. However, FRET (34,40) is especially informative in the study of conformational changes of nucleic acids in solution and provides quantitative data on global structure and conformational transitions (27,41,42). In contrast to most riboswitches studied, the lysine riboswitch is especially intriguing given that it exhibits very similar structures regardless of the presence of Mg^{2+} or its cognate ligand (19,20).

We therefore introduced fluorophores in helices P1 and P5 and monitored the efficiency of FRET (E_{FRET}) between both helices (Figure 6A). In these experiments, the aptamer sequence was minimally altered to allow the introduction of fluorophores and assure the stability of the fluorescent construct. Since P1 and P5 are in close proximity in crystal structures, we predicted that the folded state would produce a large E_{FRET} value. As expected, addition of Mg^{2+} resulted in an E_{FRET} increase (Figure 6A), consistent with the location of stems P1 and P5 in the folded riboswitch structure. When the data are fitted to a simple two-state model that assumes an all-or-none conformational transition, we can calculate the magnesium ion concentration at which the transition is half complete. In the absence of lysine, the data fitted values of $[Mg^{2+}]_{1/2} = 0.5$ mM and $n = 1.3 \pm 0.1$, suggesting that the transition does not occur in a cooperative manner (Table 2). When the experiment was repeated in presence of 5 mM lysine, a different transition was observed exhibiting values of $[Mg^{2+}]_{1/2} = 0.05$ mM and $n = 0.79 \pm 0.10$, suggesting that the presence of lysine decreases the Mg^{2+} requirement by 10-fold (Table 2). These results indicate that lysine

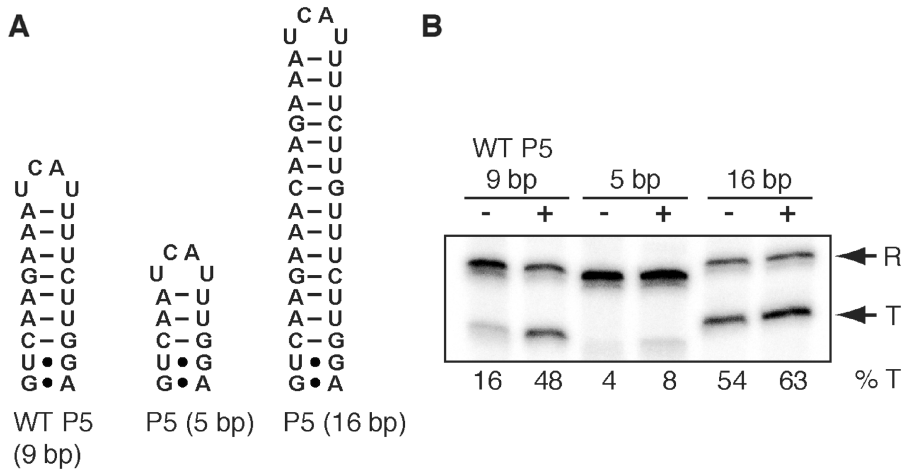

Figure 5. The P5 stem is important for lysine riboswitch activity. (**A**) Secondary structures of the 5 bp and the 16 bp P5 stem mutants. (**B**) Single-round *in vitro* transcription assays made using selected P5 riboswitch mutants in absence (–) or in presence (+) of 5 mM lysine. Reactions were performed for the wild-type riboswitch, the P5 (5 bp) and the P5 (16 bp) mutants. Readthrough (R) and prematurely terminated (T) transcripts are indicated on the right and the percentage of termination (%T) is indicated below each reaction lane.

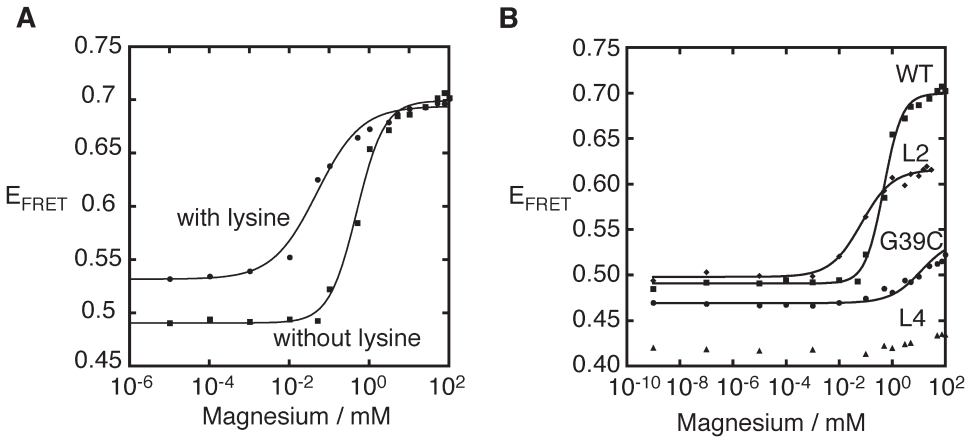

Figure 6. Lysine riboswitch folding monitored using a P1–P5 FRET vector. (**A**) Plot of the efficiency of FRET as a function of magnesium ions in the absence (squares) or the presence (circles) of 5 mM lysine. The FRET increase corresponds to a shortening of the distance between fluorophores attached to P1 and P5 stems. The data were fitted by regression to a simple two-state model in which the binding of Mg^{2+} to the aptamer induces a structural change. (**B**) Plot of the efficiency of FRET as a function of magnesium ion concentration for the WT molecule (squares), the L2 mutant (diamonds), the G39C mutant (circles) and the L4 mutant (triangles) in absence of lysine. Note that no significant change is observed when using the L4 riboswitch variant.

binding is important for the close juxtaposition occurring between P1 and P5, which is in agreement with structural probing data (17,19,20).

To determine the influence of riboswitch long-range interactions on the P1–P5 FRET transition, we introduced a series of mutations in the lysine riboswitch and studied their effects on P1–P5 folding (Figure 6B). Interestingly, the three riboswitch mutants gave distinct folding profiles. For instance, while the disruption of the L2–L3 interaction (L2 mutant) slightly altered the P1–P5 folding, the introduction of a G39C mutation significantly reduced the ability of P1 and P5 to fold (Figure 6B and Table 2). However, the disruption of the P2–L4 interaction (L4 mutant) completely abolished the folding transition, indicating that P2–L4 is crucial in the P1–P5 close juxtaposition.

The P5 stem can control the riboswitch activity

Our single-round *in vitro* transcription data show that the transcription termination is proportional to P5 stem stability (Figure 5B), which is reminiscent of our results obtained for the P1 stem (Figure 1B). Thus, given that the riboswitch activity can be modulated by altering the stability of P5, we speculated that a riboswitch construct in which the expression platform is fused to the P5 stem could control transcription termination as a function of lysine (Figure 7A). When assessing such a construct using single-round *in vitro* transcription assays, a low premature transcription of 21% was obtained in absence of lysine (Figure 7B, left panel). However, the addition of lysine resulted in a significant increase in premature termination (41%), consistent with the idea that the engineered riboswitch can modulate transcription.

Table 2. Efficiency of FRET of the P1–P5 vector for various lysine riboswitch mutants

Variant	$[Mg^{2+}]_{1/2}$ (mM)	Hill coefficient (*n*)
WT	0.50	1.3 ± 0.1
WT + lysine	0.05	0.79 ± 0.10
L2[a]	0.07	0.75 ± 0.07
L4[b]	n.d.	n.d.
G39C	2.78	0.5 ± 0.2

Half of apparent concentrations for the magnesium-induced folding process ($[Mg^{2+}]_{1/2}$) were measured under standard conditions; asymptotic standard deviations on the fits indicate that errors in ($[Mg^{2+}]_{1/2}$) are generally <10% of values; values were not determined for the L4 mutant as no significant change was observed.
[a]Nucleotides G72-G76 replaced with their Watson–Crick complement.
[b]Nucleotides A156-A157 were replaced with cytidines.

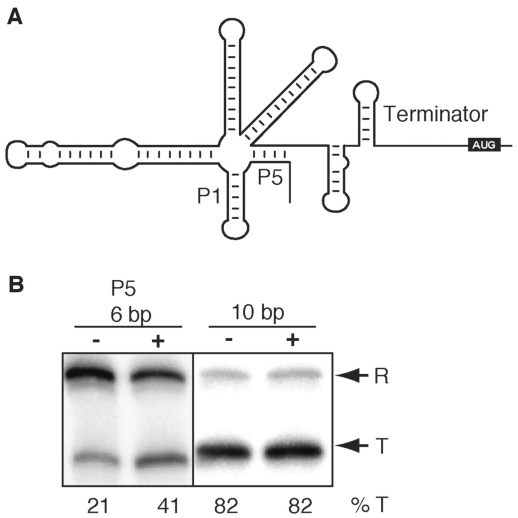

Figure 7. The P5 stem can be used as an anti-antiterminator. (**A**) Schematic of the lysine riboswitch in which the expression platform is fused to the P5 stem. (**B**) Single-round *in vitro* transcriptions were performed using constructs with a P5 stem having either 6 or 10 bp in the absence (–) and the presence (+) of 5 mM lysine. Readthrough (R) and prematurely terminated (T) transcripts are indicated on the right and the percentage of termination (%T) is indicated below each reaction lane.

Next, because the stabilization of P1 in the wild-type construct resulted in increased premature termination (Figure 1B), we speculated that the stabilization of P5 in this alternative construct should have the same effect. We thus increased the length of the P5 stem to 10 bp and used this construct in single-round transcription assays (Figure 7B, right panel). A marked increase in premature transcription termination (82%) was observed independently of lysine, indicating that the stabilization of P5 can efficiently terminate transcription prematurely. Taken together, these results support the idea that the expression platform can be relocated in different regions of the riboswitch and still allow for riboswitch activity.

The P6 stem positively influences antitermination

In this work, we have studied the importance of aptamer structural elements for the riboswitch transcription regulation. However, although the aptamer is crucial for the riboswitch function, the expression platform is also very important given that it is directly involved in genetic control (16,17,19–21). Upon examination of the *lysC* expression platform (Figure 1A), an additional stem–loop motif is found between P1 and the terminator, which we named P6. Based on the riboswitch secondary structure, the role of the P6 stem is not readily apparent as it could either be involved in the formation of the ON or OFF state. For example, P6 could be involved in a stacking interaction either with the antiterminator stem, which could stabilize the ON state, or with the terminator helix, which could favor the OFF state.

To determine if P6 has any influence on the riboswitch activity, various constructs differing in their P6 stability were engineered and used in single-round *in vitro* transcription assays (Figure 8A). When using a riboswitch in which three base pairs of the P6 stem were inhibited, thus making a 7-bp stem, a significant increase in termination was obtained both in absence (47%) and in presence of lysine (62%; Figure 8B). Higher termination efficiencies were also obtained when decreasing the P6 stem to 4 bp (≥67%) or 0 bp (≥77%). By contrast, when a more stable P6 helix (13 bp) was used, a marked reduction in termination efficiency was observed (≤14%; Figure 8B). Thus, our *in vitro* transcription data suggest that the formation of P6 stem is important for antitermination to take place, clearly suggesting a crucial role for P6 in the riboswitch function.

To assess to which extent the formation of P6 can inhibit the formation of the terminator structure, we first engineered two constructs in which the terminator stem was elongated to 12 or 14 bp. As expected, single-round transcription assays using riboswitches with either a 12- or a 14-bp terminator gave high termination efficiency (Figure 8C, left panel). When these experiments were repeated using a construct in which P6 was elongated to 13 bp, a significant decrease in transcription termination was observed when using a 12-bp terminator (Figure 8C, right panel), consistent with P6 promoting antitermination. However, no significant change was observed when the terminator was elongated to a 14 bp. Thus, these results indicate that the stability of both the P6 stem and terminator is important for the proper riboswitch regulation mechanism.

DISCUSSION

Riboswitches are exquisite RNA molecular sensors that are able to discriminate against closely similar cellular targets, which often involve the formation of high-affinity RNA–ligand complexes. Although riboswitch ligand-binding sites are constituted of highly conserved nucleotides, it is expected that less conserved peripheral elements are also important for the adoption of the native RNA structure. Perhaps one of the best examples concerning the importance of peripheral elements lies in the hammerhead ribozyme. This ribozyme has been considered for several years as a simple three-way RNA junction in which the folding pathway was entirely driven by the magnesium

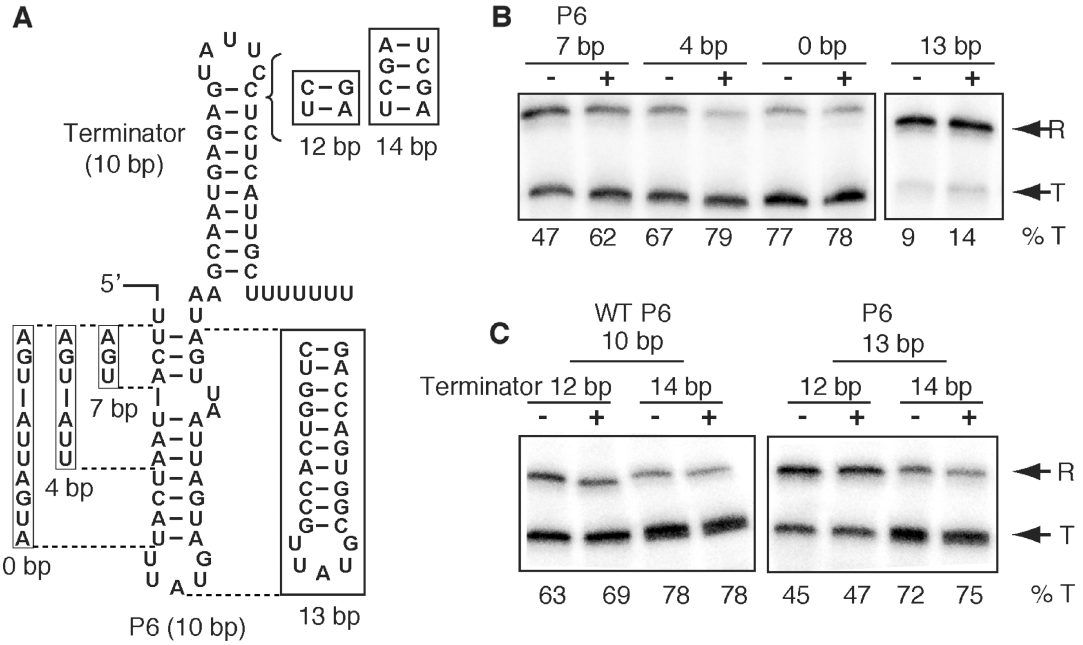

Figure 8. The structure of the P6 stem is important for transcription termination. (**A**) Secondary structure of P6 and terminator mutants. Mutated sequences for the 0-, 4- and 7-bp P6 mutants are boxed and only replace the corresponding 5′-side of P6 enclosed between dotted lines. The 13 bp P6 stem is also boxed and replaces the entire wild-type P6 stem enclosed between dotted lines. The location and the additional base pairs introduced in the terminator stem (12 and 14 bp mutants) are also shown. (**B**) Single-round *in vitro* transcription assays were made using selected P6 mutants in absence (–) or in presence (+) of 5 mM lysine. Reactions were performed for the 0-, 4-, 7- and the 13-bp P6 mutants. (**C**) Single-rounds *in vitro* transcriptions assays were made using selected terminator stem mutants in absence (–) or in the presence (+) of 5 mM lysine. Reactions were performed for the 12-bp and 14-bp terminator stem mutants either in the context of the wild-type 10 bp (left panel) or the 13 bp (right panel) P6 stem. Readthrough (R) and prematurely terminated (T) transcripts are indicated on the right and the percentage of termination (%T) is indicated below each reaction lane.

ion-dependent junction folding (43). However, recent findings have shown that a critical loop–loop interaction is important to achieve catalysis at low magnesium ion concentrations (44–46), and, importantly, the comparison of hammerhead crystal structures obtained both in the absence (47,48) and in the presence (49) of the loop–loop interaction shows that a significant structural reorganization of the hammerhead core region is caused by the formation of the tertiary interaction. This is consistent with long-range tertiary interactions being important for the folding of core regions, which is of particular interest for riboswitches as they often employ core regions to form ligand-binding sites (2).

The structure of the lysine riboswitch is defined by the presence of two long-range tertiary interactions that are proximally juxtaposed, and that are scaffolded through a five-way junction in which the lysine binding site is centrally located (Figure 1A). Recent crystal structures obtained in absence or in presence of lysine shown that tertiary interactions can be assembled independently of the ligand, suggesting that these interactions can fold the binding site at the junctional core, as we (21) and others (19,20) have shown. The work described here focuses on the role of peripheral elements on the riboswitch folding and lysine-dependent regulation control.

Importance of the P2–L4 interaction for riboswitch regulation

SHAPE data indicate that both L2–L3 and P2–L4 interactions require less magnesium ions to fold when both interactions are functional (Figure 2D and E), suggesting that the formation of each interaction can reduce the conformational space that the remaining one has to sample to fold. In a transcriptional context, the polarity of RNA polymerization suggests that L2–L3 forms first to subsequently assist in the P2–L4 formation (Figure 1A). Importantly, the P2–L4 interaction is crucial for the riboswitch core folding as revealed by 2AP fluorescence assays where no fluorescence increase was observed when altering the L4 loop sequence (Figure 4). Because 2AP is located at position 194 and that 2AP fluorescence is very sensitive to its local environment, we expect the formation of base pairs A38•G195 and G39•G193, which are in proximity to the ligand-binding site, to have a significant effect on 2AP fluorescence (Figure 9A). The marked decrease of fluorescence emission when P2–L4 is disrupted suggests that the latter is important for the correct folding of the riboswitch core region, and consequently for riboswitch activity (Figure 2B). Because core nucleotides G40 and G144 are part of stems P2 and P4, respectively, it is likely that the folding of the P2–L4 interaction is important for the correct positioning of these two nucleotides in the core region. Therefore, these results strongly suggest that P2–L4 is particularly important to organize the riboswitch ligand-binding site to ensure proper lysine-dependent riboswitch transcription activity. Our data are in agreement with previously obtained spontaneous bacterial mutants that displayed a *lysC* constitutive phenotype (24), most of which mapped to the riboswitch helical domains. These mutations very likely inhibit both

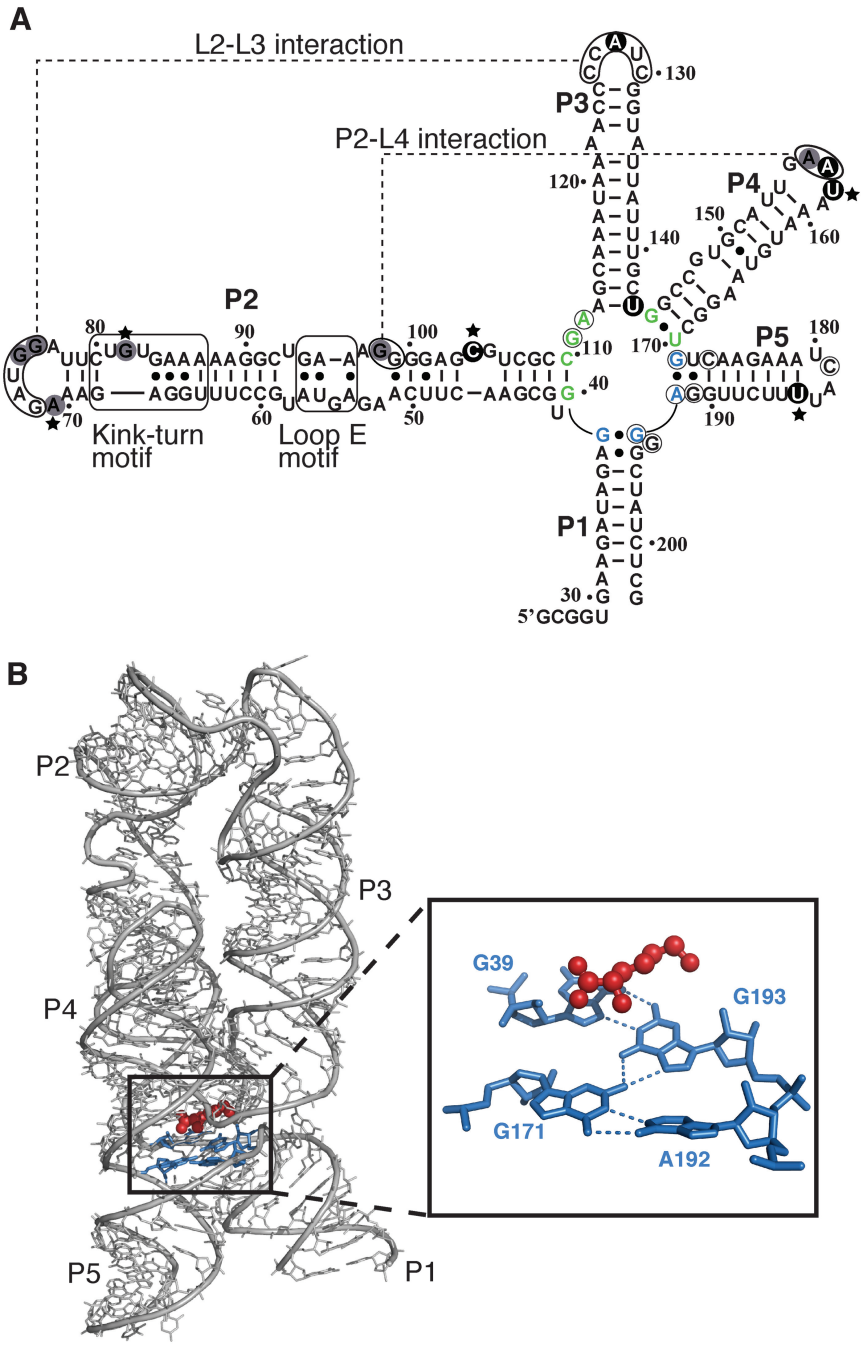

Figure 9. Folding of the lysine riboswitch as a function of magnesium ions and lysine. (**A**) Secondary structure of the lysine riboswitch summarizing NMIA reactivity obtained under different conditions. Regions involved in the formation of the kink–turn and loop E motif are boxed. L2–L3 and P2–L4 long-range tertiary interactions are indicated by dashed lines. Nucleotides reacting to NMIA upon increasing the concentration of magnesium ions or 5 mM L-lysine are indicated by black and empty circles, respectively. Nucleotides reacting in both conditions are indicated by gray circles. Nucleotides that are identified by a star show an increase in NMIA reaction. Nucleotides involved in the binding pocket and in the purine quartet are indicated in green and blue, respectively. (**B**) Representation of the lysine riboswitch crystal structure (19,20). Lysine is represented in red and nucleotides forming the purine quartet spanning stems P1 and P5 are indicated in blue. The inset shows the bottom junction layer where non-canonical base pairs G39•G193 and G171•A192 identified in blue are involved in the purine quartet. Note that numbering of the crystallized lysine riboswitch of *Thermotoga maritima* has been replaced by corresponding positions in the *lysC* lysine riboswitch of *Bacillus subtilis* (21).

L2–L3 and P2–L4 tertiary interactions, thus precluding riboswitch activity. However, even if mutations disabling the P2–L4 tertiary interaction have significant impacts on both global structure and riboswitch activity, such mutants still display limited lysine-induced effects on transcription termination (Figure 2B and ref. 21). By contrast, the binding mutant G39C does not have any impact on global folding of the RNA (Figure 3A), but sufficiently disrupts local folding of the riboswitch binding pocket (Figure 4) to completely inhibit ligand

binding (Figure 3C and ref. 21). These results are in good agreement with previous reports that identified *lysC* riboswitch mutants at nucleotide position 39 that were resistant to the lysine analog AEC (23,38). One reason for the absence of a lysine-induced riboswitch regulation in the context of a G39C mutant could be that C39 interacts with G111, which would perturb the riboswitch core as observed by 2AP fluorescence. Moreover, such interaction could readily destabilize the P1 stem, thus leading to the complete absence of response to lysine in transcription regulation.

The lysine riboswitch aptamer exhibits a P1–P5 folding transition

The P5 helix is one of the least conserved elements of the aptamer and according to sequence alignments, the length of P5 can vary from 4 bp to more than 15 bp (16,17,50). Although no obvious role for P5 can be deduced from alignments, crystal structures show that P5 stacks onto the P4 stem and lies in close proximity to P1, suggesting that P5 could be important for P1 stabilization and riboswitch regulation. Transcription assays show that the stability of P5 is important for riboswitch function (Figure 5B), and as deduced from FRET transitions (Figure 6A), the close juxtaposition between P1 and P5 is Mg^{2+}-dependent and occurs in the low mM range, similar to what we observed from SHAPE experiments for the folding of interactions L2–L3 and P2–L4 (Figure S1B). Interestingly, the presence of lysine decreases the Mg^{2+} requirement by 10-fold, suggesting the involvement of lysine in the riboswitch folding. According to the crystal structure, interactions G39•G193 and G171•A192 are part of P1 and P5, respectively, and are involved in the formation of a purine quartet that is located underneath the bound lysine (Figure 9B). The structural relationship between the formation of the quartet and P1–P5 folding transition will require additional efforts. For instance, it will be crucial to understand if the P1–P5 transition observed by FRET is important for the creation of this quartet, the latter being highly likely required for lysine binding. SHAPE analysis also show that the presence of lysine facilitates the folding of the riboswitch (Figure 3B), suggesting that ligand binding stabilizes the folded state of the lysine riboswitch (Figure 9A and B).

Although the nature of the FRET transition could purely result from a translational movement of one helix, a mixed nature involving translation and helical rotation could also produce the observed FRET increase. For instance, Batey and co-workers (20) observed that one of the main differences between lysine riboswitch crystals obtained in the absence or presence of lysine lies in the rotational orientation of the 5′-side of the P1 helix. Nevertheless, our results are consistent with the P1–P5 FRET transition being highly dependent on the correct formation of the P2–L4 interaction, suggesting that P2–L4 assists the P1–P5 folding transition most probably through the P4–P5 stacking interaction.

The P5 stem can act as an anti-antiterminator to control riboswitch activity

Very little information is available on the relative importance of the expression platform for riboswitch regulation. Our transcription assays indicate that P1 length is optimal for the *lysC* riboswitch and that the riboswitch system is very tight since the addition or the removal of only 2 bp significantly disrupts the ligand-induced transcription attenuation, without completely preventing ligand binding (data not shown). The addition of 2 bp is predicted to result in a $\Delta\Delta G^{\circ}_{37}$ of -4.7 kcal/mol (51), a value which agrees well with those of -8.3 kcal/mol and -7.6 kcal/mol that were obtained for the binding to the adenine riboswitch of 2AP (52) and adenine (53), respectively. Interestingly, examination of a recently published lysine riboswitch sequence alignment shows that an important number of P1 stem sequences vary not only in their length (54), but also in their Watson–Crick base pair ratio as various mismatches are found in the P1 helical domain, suggesting that the stability of P1 stems may be used to fine-tune the gene expression regulation. Our observations about the importance of the P1 stem sequence for the riboswitch activity are consistent with previous findings (16).

In our transcription assays, we also observed that the stability of the P5 stem is important for the riboswitch function (Figure 5). In our constructs, if we consider the P5 helical domain independently of the rest of the riboswitch molecule, the use of a P5 stem consisting of 5 bp and of 16 bp corresponds to a $\Delta\Delta G^{\circ}_{37}$ of 6.3 kcal/mol and -11.5 kcal/mol, respectively, compared to the wild-type molecule. Because of the correlation between P5 stabilities and transcription regulation, we speculated that P5 could replace P1 as the anti-antiterminator. Although lysine-dependent transcription attenuation is not as efficient as what we obtained in the context of the wild-type molecule (Figure 7B), a riboswitch activation of 2-fold observed in the presence of lysine suggests that a re-engineered riboswitch harboring an expression platform fused to P5 still displays a lysine-induced stabilization that leads to a premature transcription termination. This suggests that the riboswitch activity can also be controlled by using P5 as an anti-antiterminator. Interestingly, nucleotides G195–U197 are found in close proximity to the P5 stem. Because these nucleotides are located in the 3′ strand of the P1 stem, it is possible that the presence of P5 may influence the stability of the P1 stem. A nearly identical configuration is present in the SAM-I riboswitch (55) where natural variations in P4 stem also influence ligand-induced gene regulation (Heppell,B. *et al.*, in preparation), suggesting that the use of nonconserved helical domains may be a common feature employed by riboswitches to stabilize the P1 stem in the ligand-bound conformation. The successful relocation of the expression platform to the P5 helical domain shows an additional level of riboswitch modularity, best exemplified by the TPP riboswitch that is found in various expression platform configurations to regulate different biological process, such as transcription, translation, mRNA splicing and stability (1).

The P6 stem is important for the riboswitch regulatory activity

The formation of the stem–loop P6 was found to be important for the lysine riboswitch activity (Figure 8B). Although its position within the expression platform could not readily provide information about its functional role, the latter is consistent with the transcription polarity of the riboswitch where secondary structure elements should fold as they are transcribed. Thus, in the case of the lysine riboswitch, given that P6 and the antiterminator sequences are located proximally, it is likely that both elements are involved in the formation of a large antiterminator helical domain that is required for an efficient riboswitch regulation. Given that the P6 stem is not conserved among lysine riboswitches (18), it is probable that the sequence of P6, and also of the terminator, have evolved for efficient gene regulation in various cellular contexts, agreeing well with our results showing that the addition or the removal of two or three base pairs in either domain is clearly detrimental for riboswitch activity (Figure 8).

The high specificity that riboswitches display toward their cognate ligand is mainly associated to the proper organization of the core domain, which is well illustrated by the conservation of involved nucleotides. Our results highlight the importance of long-range interactions for the formation of the ligand-binding site as these elements have to be precisely positioned to ensure efficient ligand binding and riboswitch activity. The importance of peripheral elements for riboswitches is likely to be found in other riboswitch families, as recently observed (56).

SUPPLEMENTARY DATA

Supplementary Data are available at NAR Online.

ACKNOWLEDGEMENTS

We thank members of the Lafontaine laboratory for discussion, Simon Fournier for technical assistance, Dr. Alain Lavigueur for critical reading of the manuscript.

FUNDING

The Natural Sciences and Engineering Research Council of Canada (NSERC). S.B. holds a doctoral fellowship from NSERC and D.A.L. is a Canadian Institutes of Health Research (CIHR) New Investigator scholar as well as a Chercheur–boursier Junior 2 from the Fonds de la recherche en Santé du Québec (FRSQ). Funding for open access charge: The Natural Sciences and Engineering Research Council of Canada (NSERC).

Conflict of interest statement. None declared.

REFERENCES

1. Serganov,A. and Patel,D.J. (2007) Ribozymes, riboswitches and beyond: regulation of gene expression without proteins. *Nat. Rev. Genet.*, **8**, 776–790.
2. Roth,A. and Breaker,R.R. (2009) The structural and functional diversity of metabolite-binding riboswitches. *Annu. Rev. Biochem.*, **78**, 305–334.
3. Edwards,T.E., Klein,D.J. and Ferre-D'Amare,A.R. (2007) Riboswitches: small-molecule recognition by gene regulatory RNAs. *Curr. Opin. Struct. Biol.*, **17**, 273–279.
4. Schwalbe,H., Buck,J., Furtig,B., Noeske,J. and Wohnert,J. (2007) Structures of RNA switches: insight into molecular recognition and tertiary structure. *Angew. Chem. Int. Ed. Engl.*, **46**, 1212–1219.
5. Cromie,M.J., Shi,Y., Latifi,T. and Groisman,E.A. (2006) An RNA sensor for intracellular Mg(2+). *Cell*, **125**, 71–84.
6. Chowdhury,S., Maris,C., Allain,F.H. and Narberhaus,F. (2006) Molecular basis for temperature sensing by an RNA thermometer. *EMBO J.*, **25**, 2487–2497.
7. Grundy,F.J. and Henkin,T.M. (2004) Regulation of gene expression by effectors that bind to RNA. *Curr. Opin. Microbiol.*, **7**, 126–131.
8. Tucker,B.J. and Breaker,R.R. (2005) Riboswitches as versatile gene control elements. *Curr. Opin. Struct. Biol.*, **15**, 342–348.
9. Gilbert,S.D. and Batey,R.T. (2006) Riboswitches: fold and function. *Chem. Biol.*, **13**, 805–807.
10. Yao,Z., Barrick,J., Weinberg,Z., Neph,S., Breaker,R., Tompa,M. and Ruzzo,W.L. (2007) A computational pipeline for high-throughput discovery of *cis*-regulatory noncoding RNA in prokaryotes. *PLoS Comput. Biol.*, **3**, e126.
11. Weinberg,Z., Barrick,J.E., Yao,Z., Roth,A., Kim,J.N., Gore,J., Wang,J.X., Lee,E.R., Block,K.F., Sudarsan,N. *et al.* (2007) Identification of 22 candidate structured RNAs in bacteria using the CMfinder comparative genomics pipeline. *Nucleic Acids Res.*, **35**, 4809–4819.
12. Kazanov,M.D., Vitreschak,A.G. and Gelfand,M.S. (2007) Abundance and functional diversity of riboswitches in microbial communities. *BMC Genomics*, **8**, 347.
13. Freyhult,E., Moulton,V. and Clote,P. (2007) Boltzmann probability of RNA structural neighbors and riboswitch detection. *Bioinformatics*, **23**, 2054–2062.
14. Puerta-Fernandez,E., Barrick,J.E., Roth,A. and Breaker,R.R. (2006) Identification of a large noncoding RNA in extremophilic eubacteria. *Proc. Natl Acad. Sci. USA*, **103**, 19490–19495.
15. Barrick,J.E., Corbino,K.A., Winkler,W.C., Nahvi,A., Mandal,M., Collins,J., Lee,M., Roth,A., Sudarsan,N., Jona,I. *et al.* (2004) New RNA motifs suggest an expanded scope for riboswitches in bacterial genetic control. *Proc. Natl Acad. Sci. USA*, **101**, 6421–6426.
16. Grundy,F.J., Lehman,S.C. and Henkin,T.M. (2003) The L box regulon: lysine sensing by leader RNAs of bacterial lysine biosynthesis genes. *Proc. Natl Acad. Sci. USA*, **100**, 12057–12062.
17. Sudarsan,N., Wickiser,J.K., Nakamura,S., Ebert,M.S. and Breaker,R.R. (2003) An mRNA structure in bacteria that controls gene expression by binding lysine. *Genes Dev.*, **17**, 2688–2697.
18. Rodionov,D.A., Vitreschak,A.G., Mironov,A.A. and Gelfand,M.S. (2003) Regulation of lysine biosynthesis and transport genes in bacteria: yet another RNA riboswitch? *Nucleic Acids Res.*, **31**, 6748–6757.
19. Serganov,A., Huang,L. and Patel,D.J. (2008) Structural insights into amino acid binding and gene control by a lysine riboswitch. *Nature*, **455**, 1263–1267.
20. Garst,A.D., Heroux,A., Rambo,R.P. and Batey,R.T. (2008) Crystal structure of the lysine riboswitch regulatory mRNA element. *J. Biol. Chem.*, **283**, 22347–22351.
21. Blouin,S. and Lafontaine,D.A. (2007) A loop-loop interaction and a K-turn motif located in the lysine aptamer domain are important for the riboswitch gene regulation control. *RNA*, **13**, 1256–1267.
22. Blount,K.F., Wang,J.X., Lim,J., Sudarsan,N. and Breaker,R.R. (2007) Antibacterial lysine analogs that target lysine riboswitches. *Nat. Chem. Biol.*, **3**, 44–49.
23. Lu,Y., Shevtchenko,T.N. and Paulus,H. (1992) Fine-structure mapping of *cis*-acting control sites in the lysC operon of *Bacillus subtilis*. *FEMS Microbiol. Lett.*, **71**, 23–27.
24. Patte,J.C., Akrim,M. and Mejean,V. (1998) The leader sequence of the *Escherichia coli* lysC gene is involved in the regulation of LysC synthesis. *FEMS Microbiol. Lett.*, **169**, 165–170.

25. Milligan,J.F., Groebe,D.R., Witherell,G.W. and Uhlenbeck,O.C. (1987) Oligoribonucleotide synthesis using T7 RNA polymerase and synthetic DNA templates. *Nucleic Acids Res.*, **15**, 8783–8798.
26. Pleiss,J.A., Derrick,M.L. and Uhlenbeck,O.C. (1998) T7 RNA polymerase produces 5′ end heterogeneity during in vitro transcription from certain templates. *RNA*, **4**, 1313–1317.
27. Lemay,J.F., Penedo,J.C., Tremblay,R., Lilley,D.M. and Lafontaine,D.A. (2006) Folding of the adenine riboswitch. *Chem. Biol.*, **13**, 857–868.
28. Lafontaine,D.A., Wilson,T.J., Zhao,Z.Y. and Lilley,D.M. (2002) Functional group requirements in the probable active site of the VS ribozyme. *J. Mol. Biol.*, **323**, 23–34.
29. Clegg,R.M., Murchie,A.I., Zechel,A., Carlberg,C., Diekmann,S. and Lilley,D.M. (1992) Fluorescence resonance energy transfer analysis of the structure of the four-way DNA junction. *Biochemistry*, **31**, 4846–4856.
30. Murchie,A.I., Clegg,R.M., von Kitzing,E., Duckett,D.R., Diekmann,S. and Lilley,D.M. (1989) Fluorescence energy transfer shows that the four-way DNA junction is a right-handed cross of antiparallel molecules. *Nature*, **341**, 763–766.
31. Merino,E.J., Wilkinson,K.A., Coughlan,J.L. and Weeks,K.M. (2005) RNA structure analysis at single nucleotide resolution by selective 2'-hydroxyl acylation and primer extension (SHAPE). *J. Am. Chem. Soc.*, **127**, 4223–4231.
32. Das,R., Laederach,A., Pearlman,S.M., Herschlag,D. and Altman,R.B. (2005) SAFA: semi-automated footprinting analysis software for high-throughput quantification of nucleic acid footprinting experiments. *RNA*, **11**, 344–354.
33. Winkler,W.C., Nahvi,A., Roth,A., Collins,J.A. and Breaker,R.R. (2004) Control of gene expression by a natural metabolite-responsive ribozyme. *Nature*, **428**, 281–286.
34. Lilley,D.M. (1998) Folding of branched RNA species. *Biopolymers*, **48**, 101–112.
35. Silverman,S.K. and Cech,T.R. (1999) Energetics and cooperativity of tertiary hydrogen bonds in RNA structure. *Biochemistry*, **38**, 8691–8702.
36. Lemay,J.F. and Lafontaine,D.A. (2007) Core requirements of the adenine riboswitch aptamer for ligand binding. *RNA*, **13**, 339–350.
37. Heppell,B. and Lafontaine,D.A. (2008) Folding of the SAM aptamer is determined by the formation of a K-turndependent pseudoknot. *Biochemistry*, **47**, 1490–1499.
38. Yamauchi,T., Miyoshi,D., Kubodera,T., Nishimura,A., Nakai,S. and Sugimoto,N. (2005) Roles of Mg(2+) in TPP-dependent riboswitch. *FEBS Lett.*, **579**, 2583–2588.
39. Vold,B., Szulmajster,J. and Carbone,A. (1975) Regulation of dihydrodipicolinate synthase and aspartate kinase in Bacillus subtilis. *J. Bacteriol.*, **121**, 970–974.
40. Forster,T. (1948) Zwischenmolekulare Energiewanderung und Fluoreszenz. *Ann. Phys.*, **2**, 55–75.
41. Lafontaine,D.A., Norman,D.G. and Lilley,D.M. (2002) The global structure of the VS ribozyme. *EMBO J.*, **21**, 2461–2471.
42. Walter,N.G., Hampel,K.J., Brown,K.M. and Burke,J.M. (1998) Tertiary structure formation in the hairpin ribozyme monitored by fluorescence resonance energy transfer. *EMBO J.*, **17**, 2378–2391.
43. Blount,K.F. and Uhlenbeck,O.C. (2005) The structure–function dilemma of the hammerhead ribozyme. *Annu. Rev. Biophys. Biomol. Struct.*, **34**, 415–440.
44. Khvorova,A., Lescoute,A., Westhof,E. and Jayasena,S.D. (2003) Sequence elements outside the hammerhead ribozyme catalytic core enable intracellular activity. *Nat. Struct. Biol.*, **10**, 708–712.
45. De la Pena,M., Gago,S. and Flores,R. (2003) Peripheral regions of natural hammerhead ribozymes greatly increase their self-cleavage activity. *EMBO J.*, **22**, 5561–5570.
46. Penedo,J.C., Wilson,T.J., Jayasena,S.D., Khvorova,A. and Lilley,D.M. (2004) Folding of the natural hammerhead ribozyme is enhanced by interaction of auxiliary elements. *RNA*, **10**, 880–888.
47. Pley,H.W., Flaherty,K.M. and McKay,D.B. (1994) Three-dimensional structure of a hammerhead ribozyme. *Nature*, **372**, 68–74.
48. Scott,W.G., Finch,J.T. and Klug,A. (1995) The crystal structure of an all-RNA hammerhead ribozyme: a proposed mechanism for RNA catalytic cleavage. *Cell*, **81**, 991–1002.
49. Martick,M. and Scott,W.G. (2006) Tertiary contacts distant from the active site prime a ribozyme for catalysis. *Cell*, **126**, 309–320.
50. Vitreschak,A.G., Rodionov,D.A., Mironov,A.A. and Gelfand,M.S. (2004) Riboswitches: the oldest mechanism for the regulation of gene expression? *Trends Genet.*, **20**, 44–50.
51. Xia,T., SantaLucia,J. Jr, Burkard,M.E., Kierzek,R., Schroeder,S.J., Jiao,X., Cox,C. and Turner,D.H. (1998) Thermodynamic parameters for an expanded nearest-neighbor model for formation of RNA duplexes with Watson–Crick base pairs. *Biochemistry*, **37**, 14719–14735.
52. Wickiser,J.K., Cheah,M.T., Breaker,R.R. and Crothers,D.M. (2005) The kinetics of ligand binding by an adenine-sensing riboswitch. *Biochemistry*, **44**, 13404–13414.
53. Greenleaf,W.J., Frieda,K.L., Foster,D.A., Woodside,M.T. and Block,S.M. (2008) Direct observation of hierarchical folding in single riboswitch aptamers. *Science*, **319**, 630–633.
54. Barrick,J.E. and Breaker,R.R. (2007) The distributions, mechanisms, and structures of metabolite-binding riboswitches. *Genome Biol.*, **8**, R239.
55. Montange,R.K. and Batey,R.T. (2006) Structure of the *S*-adenosylmethionine riboswitch regulatory mRNA element. *Nature*, **441**, 1172–1175.
56. Buck,J., Noeske,J., Wohnert,J. and Schwalbe,H. Dissecting the influence of Mg2+ on 3D architecture and ligand-binding of the guanine-sensing riboswitch aptamer domain. *Nucleic Acids Res.*, **38**, 4143–4153.